Notoginsenoside R1 ameliorates the inflammation induced by amyloid-β by suppressing SphK1-mediated NF-κB activation in PC12 cells

XIAONAN WANG, BEI LI, XIAOHONG YU, YE ZHOU, KAILE WANG and YUE GAO

Department of Geriatric Medicine, Affiliated Hangzhou First People's Hospital, Zhejiang University School of Medicine, Hangzhou, Zhejiang 310006, P.R. China

Received April 14, 2023; Accepted October 25, 2023

DOI: 10.3892/mmr.2023.13139

Abstract. Alzheimer's disease (AD) is the most common type of age-related dementia, and causes progressive memory degradation, neuronal loss and brain atrophy. The pathological hallmarks of AD consist of amyloid-β (Aβ) plaque accumulation and abnormal neurofibrillary tangles. Amyloid fibrils are constructed from Aβ peptides, which are recognized to assemble into toxic oligomers and exert cytotoxicity. The fibrillar Aβ-protein fragment 25-35 ($A\beta_{25-35}$) induces local inflammation, thereby exacerbating neuronal apoptosis. Notoginsenoside R1 (NGR1), one of the primary bioactive ingredients isolated from *Panax notoginseng*, exhibits effective anti-inflammatory and anti-oxidative activities. However, NGR1 pharmacotherapies targeting Aβ-induced inflammation and cell injury cascade remain to be elucidated. The present study investigated the effect and mechanism of NGR1 in $A\beta_{25-35}$-treated PC12 cells. NGR1 doses between 250 and 1,000 μg/ml significantly increased cell viability suppressed by 20 μM $A\beta_{25-35}$ peptide treatment. Notably, the present study demonstrated that $A\beta_{25-35}$ peptide-induced sphingosine kinase 1 (SphK1) signaling activation was reduced after NGR1 treatment, further inhibiting the downstream NF-κB inflammatory signaling pathway. In addition, administration of SphK1 inhibitor II (SKI-II), a SphK1 inhibitor, also significantly reduced $A\beta_{25-35}$ peptide-induced apoptosis and the ratio of NF-κB p-p65/p65. Furthermore, SphK1 knockdown in PC12 cells using small interfering RNA alleviated Aβ-induced cell apoptosis and inflammation, suggesting a pivotal role of SphK1 signaling in the anti-inflammatory effect of NGR1. In summary, NGR1 alleviated inflammation and apoptosis stimulated by $A\beta_{25-35}$ by inhibiting the SphK1/NF-κB signaling pathway and may be a promising agent for future AD treatment.

Correspondence to: Dr Yue Gao, Department of Geriatric Medicine, Affiliated Hangzhou First People's Hospital, Zhejiang University School of Medicine, 261 Huansha Road, Shangcheng, Hangzhou, Zhejiang 310006, P.R. China
E-mail: yuegao6715@163.com

Key words: notoginsenoside R1, amyloid-β, inflammation, sphingosine kinase 1, Alzheimer's disease

Introduction

The prevalence of neurodegenerative diseases, such as Parkinson's disease and Alzheimer's disease (AD) among elderly individuals, is increasing yearly (1). AD has been considered a global public health threat, and is the most common cause of dementia. The Global Burden of Disease study recently forecasted that the number of individuals with dementia would increase from 57.4 million cases globally in 2019 to 152.8 million cases in 2050 (2). The classical neuropathological hallmarks of AD include amyloid-β (Aβ) plaque accumulation and neuro-fibrillary tangles aggregated by hyperphosphorylated tau protein (3). In general terms, amyloid precursor protein (APP) is cleaved by β-secretase, and γ-secretase can support the generation and maturation of Aβ peptides, which range between 38 and 43 amino acids (4). Prospective studies have reported that accumulation of different species of Aβ peptides contributed to glial activation and increased release of pro-inflammatory cytokines, chemokines and reactive oxygen species, all of which induce subsequent pathological events in AD, such as neuroinflammation and oxidative stress (5,6). Aβ triggers a cascade that causes neuron death, synapse loss and further cognitive decline (7). However, the validity of advanced or ongoing anti-amyloid therapies for AD is controversial due to the inefficiency in ameliorating cognitive outcomes in patients with AD (8).

Glia and immune cell-activated neuroinflammation is initiated by Aβ deposition, leading to neuron loss and cell apoptosis (9). Sphingosine kinase (SphK) is the predominant isoform responsible for the phosphorylation of sphingosine to produce sphingosine 1-phosphate (S1P), which acts as a pivotal lipid signaling regulator in the process of cell apoptosis, senescence and inflammation (10,11). SphK1 and SphK2 are well-identified isoforms of SphK and exhibit different properties and biological outcomes due to their different intracellular localization and tissue distribution (12). Notably, activation of intracellular SphK1 promotes the generation of S1P, which is necessary for the phosphorylation of IκB kinase and activation

of the canonical NF-κB inflammatory signaling pathway (13). Emerging research has indicated underlying mechanisms and pathways of the SphK1/S1P axis involving neuroinflammation within different neurological disorders (14,15). One study revealed that SphK1 and its product S1P promoted the M1 microglia polarization and enhanced the production of pro-inflammatory cytokines in injured spinal cord tissue of rats, which ultimately amplificated the inflammation cascade, including nuclear phosphorylation of p38 MAPK and NF-κB p65 (14). However, another study demonstrated that elevated SphK1 activity in neurons restored Aβ phagocytosis of microglia and resolution of neuroinflammation via acetylation of cyclooxygenase 2 (COX2) (15). Therefore, the role and underlying mechanism of SphK1 in Aβ-related neuroinflammation remain to be fully elucidated.

Panax notoginseng is a traditional Chinese medicine with beneficial functions in promoting blood circulation and alleviating limb swelling (16). In addition, it has been used in several clinical trials to treat vascular dementia, cognitive decline and brain disorders in acute stroke (17,18). Notoginsenoside R1 (NGR1), one of the ingredients isolated from *P. notoginseng saponins (PNSs)*, has been reported to possess anti-inflammatory and anti-oxidative stress properties (19,20). Chen *et al* (19) demonstrated that NGR1 alleviated IL-1β-induced inflammation and oxidative stress *in vivo* and *in vitro* by activating the nuclear factor erythroid 2-related factor 2/heme oxygenase 1 signaling pathway. In addition, NGR1 attenuated isoflurane-induced neurological disorders, including cognitive decline, memory loss and neuroinflammation, in rats (20). Notably, NGR1 exhibited a neuroprotective effect, including increasing memory function, improving learning ability and alleviating neuronal hyperexcitability via the regulation of voltage-gated sodium channels (Nav) proteins, in a mouse model of AD (21). These existing results implied that NGR1 might exert a neuroprotective effect on AD-related neuroinflammation and other neurological injuries. However, to the best of our knowledge, the specific mechanism of NGR1 in Aβ-induced neuroinflammation in AD progression remains unclear.

Given the beneficial role of NGR1 in ameliorating AD-related neurological disorders, the present study assessed whether NGR1 treatment protects against $A\beta_{25-35}$-induced neuron apoptosis and inflammation and the underlying mechanism. The present study first examined Aβ-protein fragment 25-35 ($A\beta_{25-35}$)-induced cell apoptosis and NF-κB inflammatory signaling pathway activation in PC12 rat adrenal chromaffin cell tumor cells co-incubated with $A\beta_{25-35}$ and different concentrations of NGR1. In addition, the present study used small interfering RNA (siRNA/si) to knock down SphK1 to indicate how neuroinflammation improvement by NGR1 depended on the regulation of the SphK1/NF-κB signaling axis in PC12 cells.

Materials and methods

Experimental reagents. NGR1 (batch number B21099; purity ≥98%) was acquired from Shanghai Yuanye Biotechnology Co., Ltd. For cell treatment, NGR1 was dissolved in DMSO (MilliporeSigma) and diluted in cell culture medium to keep the DMSO content below 0.1% of the total volume of the cell culture medium The preparation of $A\beta_{25-35}$ (MilliporeSigma) has been described in our previous study (22). Briefly, $A\beta_{25-35}$ was first dissolved to a concentration of 1 mM in deionized water and then aged for 72 h at 37˚C in a humidified chamber to induce its aggregation. When apparent white flocculent aggregation occurred after incubation for 72 h, the aggregated solution was dissolved in DMSO to a concentration of 250 μM and stored at -20˚C before being added to the culture medium to examine the cell viability at the final desired concentration (range, 5-30 μM), and to perform related molecular experiments at a final concentration of 20 μM. The final concentration of DMSO in the culture medium was <0.01% (vol/vol).

Cell experiments. PC12 rat pheochromocytoma cells (The Cell Bank of Type Culture Collection of The Chinese Academy of Sciences) were maintained in Ham's F-12 medium (Gibco; Thermo Fisher Scientific, Inc.) with 5% (vol/vol) heat-inactivated FBS (Gibco; Thermo Fisher Scientific, Inc.), 15% (vol/vol) horse serum (Gibco; Thermo Fisher Scientific, Inc.) and 1% penicillin-streptomycin solution (100 U/ml penicillin and 100 μg/ml streptomycin; Gibco; Thermo Fisher Scientific, Inc.) in a humidified incubator (5% CO_2; 95% air; 37˚C). For analysis of the effects of NGR1 on $A\beta_{25-35}$-induced cell injury, PC12 cells were stimulated with 20 μM $A\beta_{25-35}$ peptide alone or combined with different concentrations of NGR1 (50, 100, 250, 500 and 1,000 μg/ml) for 24 h at 37˚C. For analysis of the effects of SphK1 inhibitor II (SKI-II) on $A\beta_{25-35}$-induced cell injury, PC12 cells were cultured with 20 μM $A\beta_{25-35}$ peptide alone or combined with 10 μM SKI-II (HY-13822; MedChemExpress) with or without NGR1 (1,000 μg/ml) for 24 h at 37˚C based on previous studies (23,24). PC12 cells incubated at 37˚C for 24 h with only culture medium were used as the control group. A schematic diagram of cell treatments is shown in Fig. 1A. Cell viability was examined using an MTT assay according to the manufacturer's instructions as previously described (25).

RNA extraction and quantitative PCR (qPCR). Total RNA from PC12 cells was isolated using Biozol reagent (Biomiga), and cDNA was synthesized using a cDNA Reverse Transcriptase Kit (Vazyme Biotech Co., Ltd.) according to the manufacturer's instructions. The temperature protocol for reverse transcription was as follows: 37˚C for 15 min and 98˚C for 5 min. qPCR was performed using SYBR Green Real-time PCR Master Mix (Vazyme Biotech Co., Ltd.) on an Eppendorf Master Cycler ep RealPlex4 (Eppendorf SE) as previously described (26). The reaction conditions were as follows: 2-min pre-denaturation at 95˚C, followed by 40 cycles of 15 sec at 95˚C and 30 sec at 60˚C. *GAPDH* was used as a housekeeping gene for data standardization. The gene expression was calculated using the $2^{-\Delta\Delta Cq}$ method as described previously (27). The primer sequences are listed in Table I.

TUNEL staining. A TUNEL BrightGreen apoptosis detection kit (Vazyme Biotech Co., Ltd.) was used to detect apoptotic cells as described in our previous study (22). Briefly, PC12 cells were cultured on coverslips until they reached 70-80% confluence. Subsequently, the PC12 cells were treated with 20 μM $A\beta_{25-35}$ peptide alone or co-incubated with different concentrations of NGR1 ranging between 50 and 1,000 μg/ml

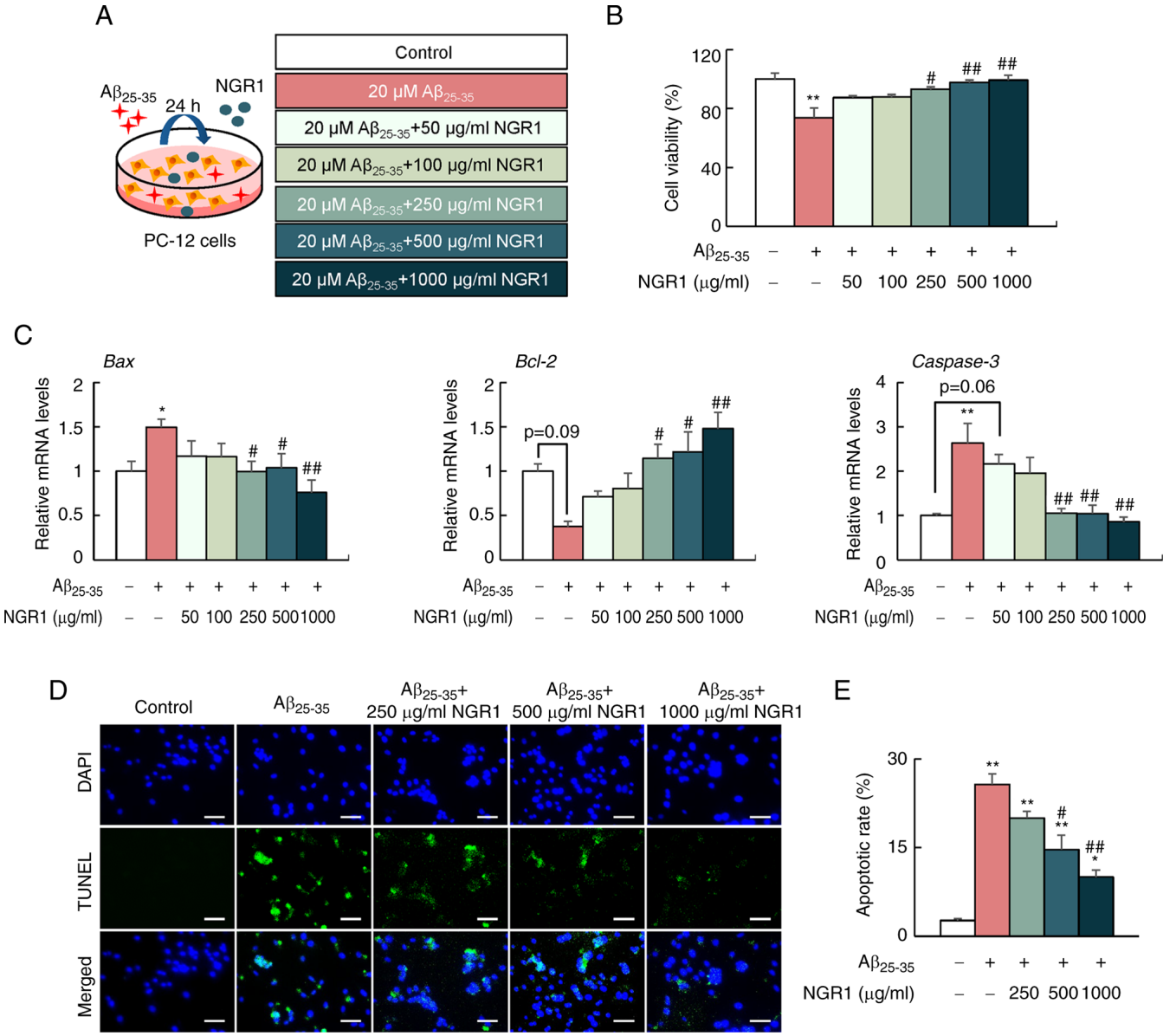

Figure 1. Effects of NGR1 on cell viability and apoptosis in PC12 cells. (A) Cell experiment design. (B) Viability of PC12 cells treated with 20 μM $A\beta_{25-35}$ and different concentrations of NGR1 for 24 h as examined using an MTT assay. n=6. (C) mRNA expression levels of *Bax*, *Bcl-2* and *Caspase3* in PC12 cells. n=6. (D) Representative confocal images of TUNEL-positive (green) apoptotic cells and DAPI-labeled nuclei (blue) of PC12 cells. Scale bar, 50 μm. n=3. (E) Apoptotic rate quantification. Data are presented as the mean ± SEM. *P<0.05, **P<0.01 vs. untreated control group; $^{\#}$P<0.05, $^{\#\#}$P<0.01 vs. 20 μM $A\beta_{25-35}$ group. $A\beta_{25-35}$, amyloid-β-protein fragment 25-35; NGR1, notoginsenoside R1.

for 24 h at 37˚C. After fixation with 4% paraformaldehyde at room temperature for 15 min and permeabilization with 0.2% Triton X-100 (MilliporeSigma) for 10 min at room temperature, the apoptotic cell nuclei were stained with green fluorescein, while all cell nuclei were labeled with blue DAPI, as observed by confocal microscopy (IX83; Olympus Corporation). The fluorescence data were analyzed and quantified using ImageJ Fiji 2.9.0 (National Institutes of Health). The apoptotic cell rate was measured as the ratio of TUNEL-positive nuclei over DAPI-stained nuclei as follows: Apoptotic rate (%)=[(number of TUNEL-positive nuclei)/(number of DAPI-stained nuclei)] x100 (%).

Immunoblotting. Proteins from PC12 cells were extracted in RIPA lysis buffer (MilliporeSigma) containing protease and phosphatase inhibitors (Roche Diagnostics). According to the manufacturer's instructions, protein concentrations were quantified using a BCA protein assay kit (Thermo Fisher Scientific, Inc.). The proteins (10 μg/lane) were equally loaded onto 10% SDS gels and transferred to methanol-prewetted PVDF membranes (MilliporeSigma). The membranes were blocked for 1 h at room temperature with a 0.2% KPL detector block (SeraCare Life Sciences; LGC Limited) and then incubated with primary antibodies at 4˚C overnight. The primary antibodies used were anti-SphK1 (cat. no. abs135525; Absin Bioscience, Inc.), anti-phospho-NF-κB p65 (Ser536) (cat. no. 3033), anti-NF-κB p65 (cat. no. 3034), GAPDH (cat. no. 2118) and β-actin (cat. no. 3700) (Cell Signaling Technology, Inc.) at a dilution of 1:1,000. After washing with tris-buffered saline with 0.1% Tween® 20 detergent, the

Table I. Primer sequences.

Name	Forward primer (5'-3')	Reverse primer (5'-3')
r. Bax	GAACTGGACAACAACATGGA	GCAAAGTAGAAAAGGGCAAC
r. Bcl-2	GGGTCATGTGTGTGGAGAG	AGCCAGGAGAAATCAAACAG
r. Caspase3	GAGCTTGGAACGCGAAGAAAA	ACACAAGCCCATTTCAGGGTA
r. SphK1	CGCCTGGGCAACACCGATAA	GGCTACATAGGGGTTTCTGG
r. MMP-3	ACCTATTCCTGGTTGCTGCT	CAGGTCTGTGGAGGACTTGT
r. MMP-9	AGTGCCCTTGAACTAAGGCT	GCCTCCACTCCTTCCTAGTC
r. GAPDH	ATGGAGAAGGCTGGGGCTCACCT	AGCCCTTCCACGATGCCAAAGTTGT

r., rat; *SphK1*, sphingosine kinase 1.

membrane was incubated with HRP anti-rabbit or -mouse antibody at a dilution ratio of 1:10,000 at room temperature for 1 h (cat. no. 7074 and 7076, Cell Signaling Technology, Inc.). The band visualization was performed used an ECL chemiluminescence kit according to the manufacturer's instructions (E422, Vazyme Biotech Co., Ltd.). The procedures of western blotting were described previously (28). The intensity of the bands in the autoradiograms was examined using ImageJ Fiji 2.9.0 (National Institutes of Health).

siRNA-mediated gene silencing and transfection. PC12 cells were maintained in 6- or 12-well plates until the cells were ~70% confluent. For SphK1 siRNA interference, the cells were transfected with 50 nM si-SphK1 or si-Control (Sangon Biotech Co., Ltd.) for 6 h at 37˚C and then incubated with 20 μM $A\beta_{25-35}$ peptide alone or co-cultured with 1,000 μg/ml NGR1 for 24 h at 37˚C. The cells in the negative control group were maintained at 37˚C for 30 h without any treatment and transfection. The si-SphK1 target sequences were as follows: 5'-GGACUUGGAGAGUGAGAAATT-3' (sense) and 5'-UUU CUCACUCUCCAAGUCCTT-3' (antisense). The scrambled si-Control sequences were as follows: 5'-UUCUCCGAACGU GUCACGUTT-3' (sense) and 5'-ACGUGACACGUUCGG AGAATT-3' (antisense). Transfection of PC12 cells with the specific siRNA against SphK1 and scrambled si-Control was performed using Lipofectamine® 3000 reagent (Invitrogen; Thermo Fisher Scientific, Inc.) in Opti-MEM (Gibco; Thermo Fisher Scientific, Inc.) as described previously (22,29).

Statistical analysis. All data are presented as the mean ± SEM. Differences among the mean values were assessed using one-way ANOVA followed by the Tukey's post hoc test using Prism 9 (Dotmatics). $P<0.05$ was considered to indicate a statistically significant difference.

Results

Effects of varying concentrations of NGR1 on the viability of PC12 cells. Previous studies have reported the cell toxicity of $A\beta_{25-35}$ peptide (10-30 μM) in PC12 and SH-SY5Y cells (30-32). Our previous study demonstrated that treatment with $A\beta_{25-35}$ peptide (10-30 μM) alone reduced the cell viability at 24, 48 and 72 h (22). Consistently, the present study demonstrated that $A\beta_{25-35}$ peptide administration contributed to a significant decrease of cell viability in the dose range of 10-30 μM at 24 h compared with the control group (Fig. S1A). No significant cell toxicity was detected in PC12 cells treated with NGR1 at concentrations ranging between 50 and 1,500 μg/ml. By contrast, 2 mg/ml NGR1 treatment for 24 h significantly decreased the cell viability (Fig. S1B). Notably, addition of NGR1 increased the suppressed cell viability caused by 20 μM $A\beta_{25-35}$ administration in a dose-dependent manner from 250 to 1,000 μg/ml after 24 h (Fig. 1B). Thus, NGR1 concentrations ranging between 250 and 1,000 μg/ml were used in subsequent experiments.

NGR1 decreases apoptosis in $A\beta_{25-35}$-treated PC12 cells. The influence of NGR1 on apoptosis-related gene expression in PC12 cells was analyzed by reverse transcription-qPCR. As shown in Fig. 1C, 20 μM $A\beta_{25-35}$ treatment significantly increased the mRNA expression levels of *Bax* and *Caspase-3*, which are classical apoptosis promoters. By contrast, the mRNA expression levels of *Bcl-2*, an essential regulator in cell apoptosis inhibition, were decreased in the $A\beta_{25-35}$-treated group compared with the control group; however, this difference was not significant (Fig. 1C). However, NGR1 supplementation (250-1,000 μg/ml) reduced the mRNA expression levels of *Bax* and *Caspase-3* but increased the mRNA expression levels of *Bcl-2* in the PC12 cells co-incubated with 20 μM $A\beta_{25-35}$ peptide at 24 h in a dose-dependent manner (Fig. 1C). In addition, TUNEL staining was performed to further verify the effect of NGR1 on apoptosis (Fig. 1D and E). $A\beta_{25-35}$ administration (20 μM) increased the percentage of TUNEL-positive cells compared with the control group (Fig. 1D and E). By contrast, NGR1 treatment (500-1,000 μg/ml) dose-dependently decreased the apoptotic cells labeled by TUNEL in the PC12 cells co-treated with $A\beta_{25-35}$ peptide (Fig. 1D and E).

NGR1 inhibits $A\beta_{25-35}$-induced SphK1/NF-κB signaling activation in PC12 cells. Intracellular SphK1 is considered to modulate NF-κB activation and is responsible for the inflammatory cascade following different inflammatory stimuli (33,34). To elucidate the anti-inflammatory mechanism of NGR1 in $A\beta_{25-35}$-treated PC12 cells, the present study examined the gene and protein expression levels of SphK1 and the ratio of NF-κB p-p65/p65 in PC12 cells co-incubated with 20 μM $A\beta_{25-35}$ and different concentrations of NGR1 (Fig. 2). As shown in Fig. 2A,

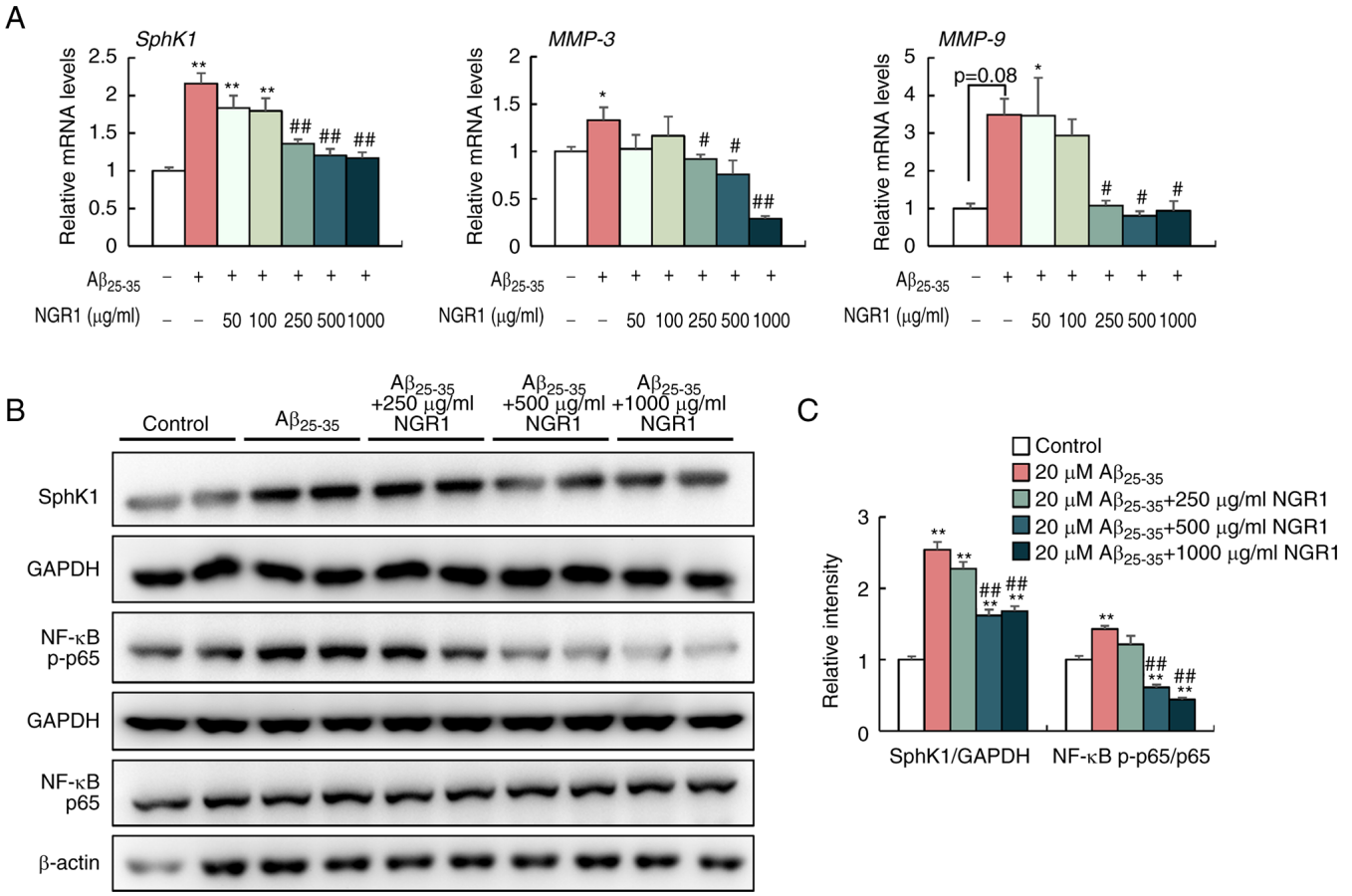

Figure 2. Effects of NGR1 on the inflammatory response in PC12 cells. (A) mRNA expression levels of *SphK1*, *MMP-3* and *MMP-9* in PC12 cells incubated with 20 μM $A\beta_{25-35}$ and different concentrations of NGR1 for 24 h. n=6. (B) Protein levels of SphK1, NF-κB p-p65 and total NF-κB p65 and their corresponding loading controls in PC12 cells. (C) Semi-quantification of the protein levels of SphK1, NF-κB p-p65 and total NF-κB p65 in PC12 cells. n=4. Data are presented as the mean ± SEM. *P<0.05, **P<0.01 vs. untreated control group; $^{\#}$P<0.05, $^{\#\#}$P<0.01 vs. 20 μM $A\beta_{25-35}$ group. $A\beta_{25-35}$, amyloid-β-protein fragment 25-35; NGR1, notoginsenoside R1; p-, phosphorylated; SphK1, sphingosine kinase 1.

$A\beta_{25-35}$ treatment increased the mRNA expression levels of *SphK1* compared with the control group, whereas NGR1 supplementation (ranging between 250 and 1,000 μg/ml) significantly reduced *SphK1* gene expression in PC12 cells. Furthermore, in a dose-dependent manner, NGR1 treatment (250-1,000 μg/ml) significantly decreased the protein levels of SphK1 and decreased the ratio of p-p65/p65 in PC12 cells compared with the 20 μM $A\beta_{25-35}$-treated group (Fig. 2B and C). Additionally, MMP-3 and MMP-9 are pivotal inflammatory components in the progression of AD, as they promote the aggregation of Aβ and tau proteins in the brain (35). Consistently, $A\beta_{25-35}$ treatment increased the mRNA expression levels of *MMP-3* and *MMP-9 in vitro*, while NGR1 administration (250-1,000 μg/ml) prominently decreased the mRNA expression levels of *MMP-3* and *MMP-9* in a dose-dependent manner (Fig. 2A).

SphK1/NF-κB signaling is involved in the anti-inflammatory effect of NGR1 in $A\beta_{25-35}$-treated PC12 cells. To clarify the role of SphK1/NF-κB signaling in the anti-inflammatory effect of NGR1 in $A\beta_{25-35}$-treated PC12 cells, 10 μM SKI-II, a SphK1 inhibitor, was co-administrated with 20 μM $A\beta_{25-35}$ peptide and 1,000 μg/ml NGR1 for 24 h (Fig. 3). SphK1 inhibition also significantly decreased the mRNA expression levels of *Bax* and *Caspase-3* but increased the mRNA expression levels of *Bcl-2* in PC12 cells to a similar extent compared with 1,000 μg/ml NGR1 supplementation compared with $A\beta_{25-35}$ treatment alone (Fig. 3A). At the same time, a decreased percentage of TUNEL-positive apoptotic cells was observed in the SKI-II-treated group and SKI-II and NGR1 group compared with the 20 μM $A\beta_{25-35}$ peptide treatment group in PC12 cells (Fig. 3B).

SphK1 inhibition by SKI-II treatment decreased the mRNA expression levels of *MMP-3* and *MMP-9* in PC12 cells compared with the $A\beta_{25-35}$ peptide-treated group (Fig. 3C). Similar to treatment with 1,000 μg/ml NGR1 and $A\beta_{25-35}$, western blotting demonstrated that SKI-II treatment significantly decreased the protein levels of SphK1 and decreased the ratio of p-p65/p65 in PC12 cells compared with those of the 20 μM $A\beta_{25-35}$ peptide-treated group (Fig. 3D and E). However, 1,000 μg/ml NGR1 and 10 μM SKI-II combined treatment did not further inhibit the activation of the NF-κB signaling pathway (Fig. 3D and E). Overall, these data illustrated the involvement of SphK1 in the inhibitory effect of NGR1 on inflammation induced by $A\beta_{25-35}$ in PC12 cells.

Knockdown of SphK1 relieves inflammation induced by $A\beta_{25-35}$ in PC12 cells. To further verify whether the activation of SphK1 mediates NGR1-alleviated inflammation, scrambled siRNA and si-SphK1 were transfected into PC12

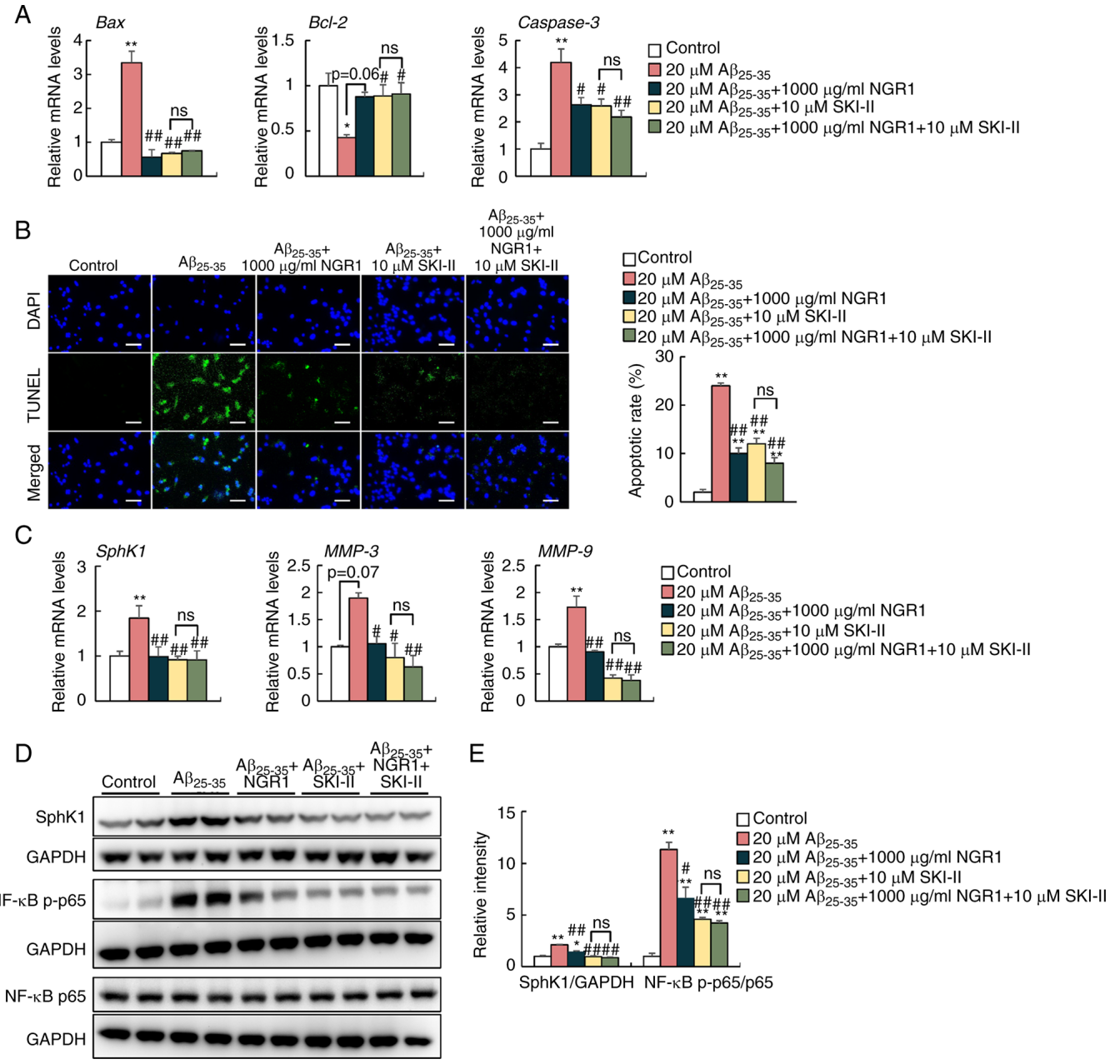

Figure 3. Effects of pharmacological inhibition of Sphk1 on $A\beta_{25-35}$-induced apoptosis and inflammation in PC12 cells. (A) mRNA expression levels of *Bax*, *Bcl-2* and *Caspase3* in PC12 cells treated with 20 μM $A\beta_{25-35}$ and 1,000 μg/ml NGR1 with or without 10 μM SKI-II. n=6. (B) Representative confocal images and apoptotic rate quantifications of TUNEL-positive (green) apoptotic cells and DAPI-labeled nuclei (blue) of PC12 cells. Scale bar, 50 μm. n=3. (C) mRNA expression levels of *SphK1*, *MMP-3* and *MMP-9* in PC12 cells. n=6. (D) Protein levels of SphK1, NF-κB p-p65 and total NF-κB p65 in PC12 cells. (E) Semi-quantification of the protein levels of SphK1, NF-κB p-p65 and total NF-κB p65 and their corresponding loading controls in PC12 cells. n=4. Data are presented as the mean ± SEM. *P<0.05, **P<0.01 vs. untreated control group; $^{\#}$P<0.05, $^{\#\#}$P<0.01 vs. 20 μM $A\beta_{25-35}$ group. $A\beta_{25-35}$, amyloid-β-protein fragment 25-35; NGR1, notoginsenoside R1; ns, not significant; p-, phosphorylated; SKI-II, SphK1 inhibitor II; SphK1, sphingosine kinase 1.

cells separately, and an untreated and untransfected negative control group was established (Figs. 4 and S2), and SphK1 was knocked down (Fig. S2). As shown in Fig. 4A, SphK1 knockdown decreased mRNA expression levels of *Bax* and *Caspase-3*, and increased mRNA expression levels of *Bcl-2* in PC12 cells compared with cells treated with $A\beta_{25-35}$ alone in the si-Control group, which indicated that SphK1 knockdown abolished the apoptosis induced by $A\beta_{25-35}$. Consistently, a decreased proportion of TUNEL-labeled apoptotic cells was observed in the 20 μM $A\beta_{25-35}$-treated si-SphK1 group when compared with the 20 μM $A\beta_{25-35}$-treated si-Control group (Fig. 4B). In addition, SphK1 knockdown significantly decreased the mRNA expression levels of *MMP-3* and *MMP-9* and decreased the ratio of p-p65/p65 in PC12 cells compared with the 20 μM $A\beta_{25-35}$-treated si-control group (Fig. 4C-E). However, knockdown of SphK1 combined with $A\beta_{25-35}$ and NGR1 treatment did not exert an effect on mRNA expression levels of *Bax*, *Caspase-3* and *Bcl-2*, and the proportion of TUNEL-stained apoptotic cells compared with combination treatment of NGR1 and $A\beta_{25-35}$ in the si-control groups (Fig. 4A and B). In addition, knockdown of SphK1 combined with $A\beta_{25-35}$ and NGR1 treatment also

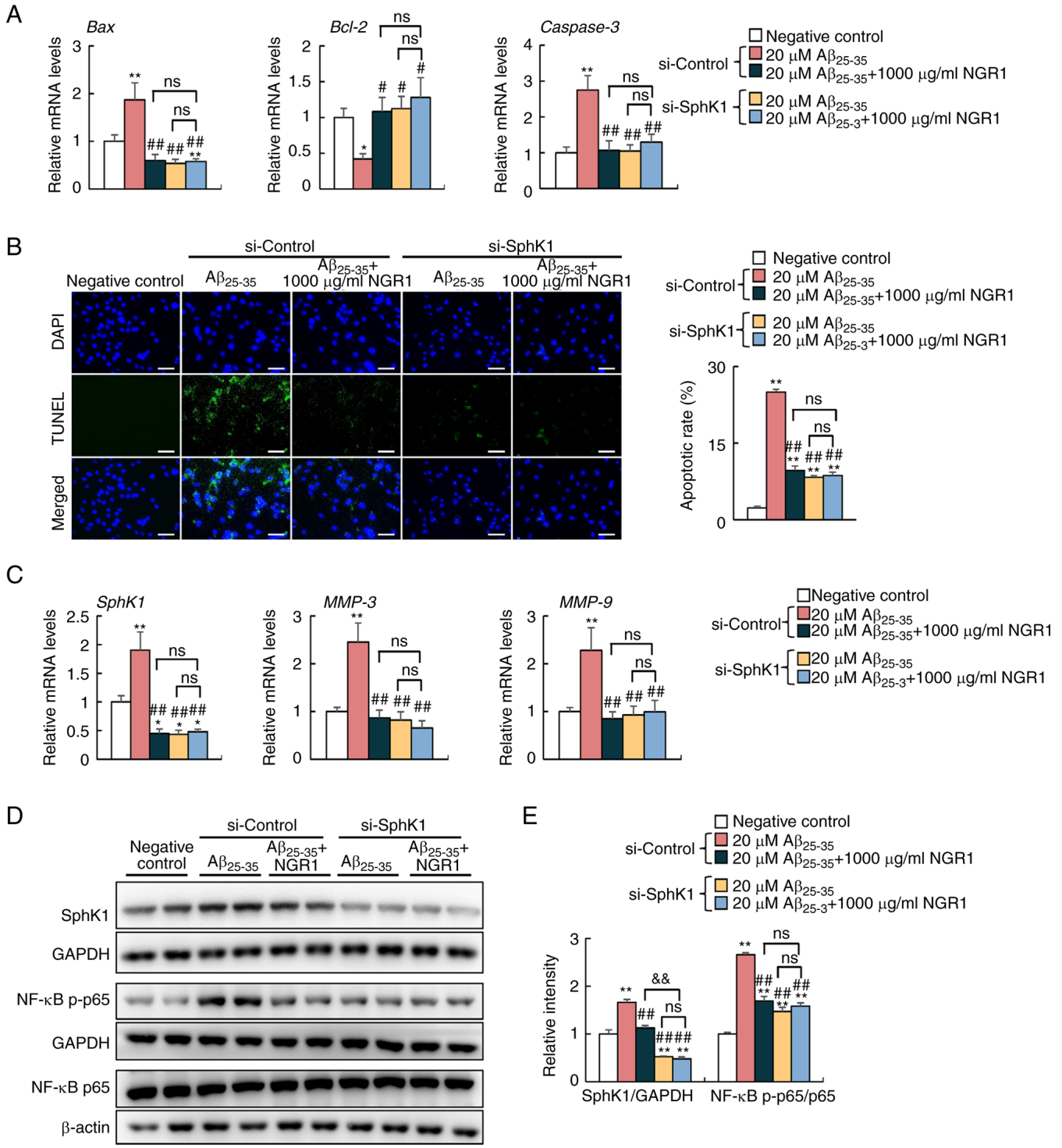

Figure 4. Effects of siRNA-mediated knockdown of Sphk1 on $A\beta_{25-35}$-induced apoptosis and inflammation in PC12 cells. (A) mRNA expression levels of *Bax*, *Bcl-2* and *Caspase3* in PC12 cells transfected with si-Control and si-Sphk1. N=6. (B) Representative confocal images and apoptotic rate quantifications of TUNEL-positive (green) apoptotic cells and DAPI-labeled nuclei (blue) of PC12 cells. Scale bar, 50 μm. N=3. (C) mRNA expression levels of *SphK1*, *MMP-3* and *MMP-9* in PC12 cells. N=6. (D) Protein levels of SphK1, NF-κB p-p65 and total NF-κB p65 and their corresponding loading controls in PC12 cells. (E) Semi-quantification of the protein levels of SphK1, NF-κB p-p65 and total NF-κB p65 in PC12 cells. n=4. Data are presented as the mean ± SEM. *P<0.05, **P<0.01 vs. negative control (no treatment or transfection); $^{\#}$P<0.05, $^{\#\#}$P<0.01 vs. si-control + 20 μM $A\beta_{25-35}$ group; $^{\&\&}$P<0.01 vs. si-control + 20 μM $A\beta_{25-35}$ + 1,000 μg/ml NGR1group. $A\beta_{25-35}$, amyloid-β-protein fragment 25-35; NGR1, notoginsenoside R1; ns, not significant; p-, phosphorylated; siRNA/si, small interfering RNA; SphK1, sphingosine kinase 1.

decreased the mRNA level of *MMP-3* and *MMP-9* and inhibited NF-κB p65 activation compared with those of the PC12 cells treated with $A\beta_{25-35}$ alone in the si-Control group, but to a similar extent compared with combined treatment with NGR1 and $A\beta_{25-35}$ in the si-control group (Fig. 4C-E). However, these data demonstrated that knockdown of SphK1 could effectively suppress Aβ-induced apoptosis and inflammation in PC12 cells.

Discussion

The principal cellular characteristic of AD is Aβ-related neurotoxicity that prompts apoptosis, which is responsible for extensive neuronal degeneration and loss in the brain (36). Although ongoing clinical trials for AD therapies that target the degradation of Aβ deposition have been unsatisfactory, widespread research has indicated high toxicity of soluble Aβ oligomers (37). In general, $A\beta_{1-40}$ and $A\beta_{1-42}$ are the most abundant species of Aβ peptides, of which $A\beta_{1-42}$ has been detected as the primary component in amyloid plaque depositions in patients with AD (38). Among the Aβ fragments available at present, the $A\beta_{25-35}$ peptide consisting of 11 amino acid residues has been found in the in the brain of patients with AD (39). In addition, a comparison study demonstrated that both $A\beta_{1-42}$ and $A\beta_{25-35}$ induced similar cell toxicity in organotypic hippocampal slices. Nevertheless, the authors highlighted that synthetic $A\beta_{25-35}$ peptide was convenient for clarifying the neurotoxic mechanisms involved in the pathogenesis of AD (40). $A\beta_{25-35}$ peptide is a cheap and convenient alternative in the pathological investigations of AD, since this smaller peptide retains the toxicity of the full-length peptide and induces a vast amount of neuron death (41). Furthermore, the $A\beta_{25-35}$ peptide forms a series of β-barrel aggregates and a dominant hexamer structure, the C terminus region of which provides the most potent interactions between two $A\beta_{25-35}$ monomers (42). Notably, aging aggravates the release of soluble $A\beta_{1-40}$ from plaques and $A\beta_{1-40}$ is converted by proteolysis to toxic $A\beta_{25-35/40}$, which causes detrimental damage in the hippocampal CA1 neurons to promote neurotoxicity in AD (39). Collectively, the present study used the $A\beta_{25-35}$ peptide as a potent inducer to simulate cell toxicity and apoptosis, effectively mimicking the pathological conditions associated with AD *in vitro*.

PC12 cells are derived from the adrenal medulla of a rat with pheochromocytoma and are widely utilized as a neuronal precursor cell line in neuroscience research (43). PC12 cells exhibit morphological and physiological traits resembling those of adrenal gland cells in the undifferentiated state (43). These cells are commonly employed in numerous studies to investigate the neurotoxic effects of various substances (44,45). For instance, PC12 cells are frequently used to study Aβ-induced neurotoxicity, as an *in vitro* model simulating aspects of AD (46). Our previous study revealed that the $A\beta_{25-35}$ peptide markedly contributed to severe apoptosis and oxidative stress in PC12 cells (22). A recent study also revealed that $A\beta_{25-35}$ administration enhanced apoptosis and activated the NF-κB signaling pathway in an APP/presenilin 1 double-transgenic mouse model of AD and BV2 microglia cell line (47). Consistent with these previous findings, the present study used $A\beta_{25-35}$ peptide to establish AD-related phenotypes in PC12 cells, including cellular apoptosis and neuroinflammation. In the present study, 20 μM $A\beta_{25-35}$ treatment for 24 h was used and significantly induced apoptosis, as demonstrated by the decrease in cell viability, increased mRNA expression levels of pro-apoptotic markers (*Bax* and *Caspase3*) and increased percentage of TUNEL-labeled apoptotic cells. In addition, $A\beta_{25-35}$ markedly activated the NF-κB inflammatory signaling pathway associated with the increased levels of Sphk1 signaling in PC12 cells. Notably, the present study demonstrated that NGR1 blocked the NF-κB inflammatory pathway by inhibiting SphK1 signaling, thereby reversing $A\beta_{25-35}$-induced apoptosis and inflammatory damage in PC12 cells. However, a limitation of the present study was the absence of protein detection of cleaved caspase3, necessitating further investigations to conclusively ascertain the impact of NGR1 on apoptosis.

Prospective studies have demonstrated the advantages of *P. notoginseng* in alleviating inflammation, inhibiting cell apoptosis and reducing thrombosis (48,49). As the bioactive component of *P. notoginseng*, PNS exhibits neuroprotective effects on the progression of AD by inhibiting Aβ production and aggregation and alleviating inflammation (50). Notably, NGR1, a primary active ingredient of *PNSs*, has also been reported to have beneficial effects on neuronal activity repairment in AD development (51,52). For instance, oral administration of NGR1 effectively improved Aβ-induced synaptic plasticity deficits in brain slices and reduced Aβ neurotoxicity by recovering $A\beta_{1-42}$ oligomer-induced long-term potentiation impairment (51). Hu *et al* (21) demonstrated that NGR1 treatment restored cell viability of primary cultured mouse neurons after $A\beta_{1-42}$ administration and reduced neuronal hyperexcitability via the reallocation of Nav1.1α and prevention of excessive cleavage of Navβ2. The present findings demonstrated that NGR1 supplementation increased viability in a dose-dependent manner after incubation of PC12 cells with $A\beta_{25-35}$ and decreased apoptosis. Another study also demonstrated that NGR1 counteracted the cell damage induced by $A\beta_{25-35}$ by increasing cell viability, alleviating cellular oxidative damage and normalizing mitochondrial membrane potential via the suppression of the MAPK signaling pathway in PC12 cells (52). Therefore, we hypothesized that NGR1 exerted neuroprotective effects against $A\beta_{25-35}$-induced cell injury by alleviating apoptosis in PC12 cells.

Extracellular Aβ deposition indicates neurotoxicity resulting in neuronal death, microglia activation and excessive production of pro-inflammatory cytokines, which are mediated through binding to neurotrophic factors, such as N-methyl-D-aspartate receptor and insulin receptor (53). The present study revealed activation of the NF-κB inflammatory signaling pathway in $A\beta_{25-35}$-treated PC12 cells. In addition, in the present study, $A\beta_{25-35}$ treatment markedly increased the mRNA expression levels of MMP-3 and MMP-9, which are located around amyloid plaques and elevated in the brain of patients with AD (54,55). In the Ra2 microglia cell line, excessive Aβ accumulation elevated the activity of MMP-3 and subsequently activated PI3K/Akt signaling inflammatory cascades (56). In addition, the simultaneous accumulation of cortical MMP-9 may be recognized as a pathological marker of the early onset of AD (57), and MMP-3 has been demonstrated to activate MMP-9 effectively and to indirectly facilitate AD pathology (58). The present study revealed inhibition of phosphorylation of NF-κB p65 and decreased mRNA expression levels of MMP-3 and MMP-9 in NGR1-treated groups compared with the group treated with only $A\beta_{25-35}$. Although the substantial role and mechanism of MMP-3 and MMP-9 in the Aβ-induced inflammatory response remain elusive, the present data suggested that MMP-3 and MMP-9 were involved in the $A\beta_{25-35}$-related neurotoxicity and

inflammation. Therefore, further investigation is required to examine the potential role and possible mechanism of MMPs in the Aβ neurotoxicity during AD progression.

In addition to the downregulation of NF-κB activation, the present study also revealed a marked decrease in SphK1 mRNA and protein expression in NGR1-treated groups. SphK1 is one of the rate-limiting enzymes catalyzing S1P generation, which subsequently binds to a series of intracellular S1P receptors and is involved in various inflammatory diseases (11). One study reported that SphK1 and its product S1P acted as viable therapeutic targets for mediating neuroinflammation via the phosphorylation of p38 MAPK and ultimate activation of NF-κB p65 (14). Conversely, treatment with PF543, a validated inhibitor of SphK1, reversed pro-inflammatory M1-type microglia-facilitated neuron apoptosis and NF-κB p65 activation in PC12 cells (14). Consistently, the present data demonstrated that NGR1 decreased the mRNA and protein levels of SphK1 and inhibited the phosphorylation level of NF-κB p65. The present study used 10 μM SKI-II as an effective SphK1 inhibitor (23,24). It demonstrated that pharmacological inhibition of SphK1 markedly decreased apoptosis and decreased the ratio of p-p65/p65 in PC12 cells. A prior study of the pharmacokinetics of SKI-II suggested a pro-inflammatory effect in atherosclerosis-prone mice (59). However, to the best of our knowledge, the role of the SphK1-triggered inflammatory signaling pathway in Aβ toxicity has not been fully elucidated. In the present study, pharmacological inhibition by SKI-II administration and siRNA-mediated SphK1 knockdown were performed in PC12 cells. Notably, the present study revealed significant alleviation of $A\beta_{25-35}$-induced apoptosis and the NF-κB inflammatory response when SphK1 was inhibited or knocked down. However, the underlying mechanism of SphK1 signaling appears to be complicated and controversial in Aβ neurotoxicity (24). In APP-transfected PC12 cells, the presence of endogenous Aβ peptides led to a reduction in SphK1 activity, and treatment with SKI-II decreased cell viability (24). In addition, a reduction of SphK1 activity was observed in the neurons of patients with AD and mice (60), while COX2 acetylated by the activated SphK1 signaling contributed to the resolution of neuroinflammation and Aβ phagocytosis by microglia in AD (15). Furthermore, glial cells, mainly microglia, and astrocytes are involved in the pathogenesis of AD by regulating the phagocytosis of Aβ proteins and the release of pro-inflammatory cytokines (61). Therefore, further investigations involving the concrete mechanism regarding NGR1 and $A\beta_{25-35}$-activated neuroinflammation and subsequent glial cell activation via SphK1 signaling are required. Notably, the increased mRNA expression levels of MMP-3 and MMP-9 following treatment with $A\beta_{25-35}$ were decreased when SphK1 was inhibited or knocked down. Although few studies have focused on the role of SphK1 in $A\beta_{25-35}$-related neurotoxicity via the regulation of MMP-3 and MMP-9, the activity of S1P, a downstream product of SphK1, elevated the levels of MMP-3 and subsequently promoted the progression of osteoarthritis (62). In addition, N, N-dimethylsphingosine, a potent SphK1 inhibitor, also decreased the levels of MMP-9 and other pro-inflammatory cytokines in the cellular junctions between Jurkat-U937 cells and rheumatoid arthritis human peripheral blood mononuclear cells (63). Therefore, SphK1-regualted MMP-3 and MMP-9 may be a potential mechanism for investigating $A\beta_{25-35}$-related neurotoxicity and the inflammatory response. Notably, the inhibition of SphK1 in PC12 cells did not result in any alterations in the mRNA expression levels of MMP-3 or MMP-9, nor did it affect the ratio of p-p65/p65 compared with those of cells treated with NGR1 and $A\beta_{25-35}$. These findings suggested that the SphK1-mediated activity of MMP-3 and MMP-9 may serve a role in the NGR1-related neuroprotective effect on $A\beta_{25-35}$-induced neurotoxicity and inflammation.

Taken together, the present study revealed that NGR1 supplementation increased the viability and protected PC12 cells against $A\beta_{25-35}$-induced apoptosis in a dose-dependent manner. Furthermore, NGR1 treatment alleviated the $A\beta_{25-35}$-activated inflammatory response by inhibiting SphK1-mediated NF-κB signaling pathway activation. These findings highlighted the neuroprotective role of NGR1 in $A\beta_{25-35}$-related neurological impairment and provided a theoretical basis for further understanding the mechanism of NGR1 in Aβ neurotoxicity.

However, a major limitation of the present study was its focus on detecting changes of apoptosis markers at the gene level without considering alterations at the protein level, which could have been detected by western blotting. Therefore, further investigations involving protein analyses are required to confirm the validity of these results. Further studies using an *in vivo* AD model and corresponding primary neuron cells are required to identify the exact role and mechanism of the SphK1 signaling in the NGR1-mediated anti-inflammatory effects during the progression of AD.

Acknowledgements

Not applicable.

Funding

The present study was supported by the Science and Technology Program of Zhejiang Traditional Chinese Medicine (grant no. 2014ZB077), Hangzhou Science and Technology development program (grant no. 20150733Q13), Zhejiang Provincial Key Laboratory of Traditional Chinese Medicine for the Prevention and Treatment of Major Chronic Diseases of the Elderly, and the Construction Fund of Key Medical Disciplines of Hangzhou (grant no. OO20200055).

Availability of data and materials

The datasets used and/or analyzed during the current study are available from the corresponding author on reasonable request.

Authors' contributions

XW, BL, XY, YZ, KW and YG collected samples, and acquired and analyzed data. XW wrote the manuscript. XW and YG contributed to the study concept, and drafted and revised the manuscript. XW and YG confirm the authenticity of all the raw data. All authors read and approved the final version of the manuscript.

Ethics approval and consent to participate

Not applicable.

Patient consent for publication

Not applicable.

Competing interests

The authors declare that they have no competing interests.

References

1. Weintraub S, Karpouzian-Rogers T, Peipert JD, Nowinski C, Slotkin J, Wortman K, Ho E, Rogalski E, Carlsson C, Giordani B, *et al*: ARMADA: Assessing reliable measurement in Alzheimer's disease and cognitive aging project methods. Alzheimers Dement 18: 1449-1460, 2022.
2. GBD 2019 Dementia Forecasting Collaborators: Estimation of the global prevalence of dementia in 2019 and forecasted prevalence in 2050: An analysis for the global burden of disease study 2019. Lancet Public Health 7: e105-e125, 2022.
3. Zetterberg H and Mattsson N: Understanding the cause of sporadic Alzheimer's disease. Expert Rev Neurother 14: 621-630, 2014.
4. Leng F and Edison P: Neuroinflammation and microglial activation in Alzheimer disease: Where do we go from here? Nat Rev Neurol 17: 157-172, 2021.
5. Del Bo R, Angeretti N, Lucca E, De Simoni MG and Forloni G: Reciprocal control of inflammatory cytokines, IL-1 and IL-6, and beta-amyloid production in cultures. Neurosci Lett 188: 70-74, 1995.
6. Akiyama H, Barger S, Barnum S, Bradt B, Bauer J, Cole GM, Cooper NR, Eikelenboom P, Emmerling M, Fiebich BL, *et al*: Inflammation and Alzheimer's disease. Neurobiol Aging 21: 383-421, 2000.
7. Busche MA and Hyman BT: Synergy between amyloid-β and tau in Alzheimer's disease. Nat Neurosci 23: 1183-1193, 2020.
8. Haass C and Selkoe D: If amyloid drives Alzheimer disease, why have anti-amyloid therapies not yet slowed cognitive decline? PLoS Biol 20: e3001694, 2022.
9. Thakur S, Dhapola R, Sarma P, Medhi B and Reddy DH: Neuroinflammation in Alzheimer's disease: Current progress in molecular signaling and therapeutics. Inflammation 46: 1-17, 2023.
10. Hofmann LP, Ren S, Schwalm S, Pfeilschifter J and Huwiler A: Sphingosine kinase 1 and 2 regulate the capacity of mesangial cells to resist apoptotic stimuli in an opposing manner. Biol Chem 389: 1399-1407, 2008.
11. Kunkel GT, Maceyka M, Milstien S and Spiegel S: Targeting the sphingosine-1-phosphate axis in cancer, inflammation and beyond. Nat Rev Drug Discov 12: 688-702, 2013.
12. Spiegel S and Milstien S: Sphingosine-1-phosphate: An enigmatic signalling lipid. Nat Rev Mol Cell Biol 4: 397-407, 2003.
13. Alvarez SE, Harikumar KB, Hait NC, Allegood J, Strub GM, Kim EY, Maceyka M, Jiang H, Luo C, Kordula T, *et al*: Sphingosine-1-phosphate is a missing cofactor for the E3 ubiquitin ligase TRAF2. Nature 465: 1084-1088, 2010.
14. Wang C, Xu T, Lachance BB, Zhong X, Shen G, Xu T, Tang C and Jia X: Critical roles of sphingosine kinase 1 in the regulation of neuroinflammation and neuronal injury after spinal cord injury. J Neuroinflammation 18: 50, 2021.
15. Lee JY, Han SH, Park MH, Song IS, Choi MK, Yu E, Park CM, Kim HJ, Kim SH, Schuchman EH, *et al*: N-AS-triggered SPMs are direct regulators of microglia in a model of Alzheimer's disease. Nat Commun 11: 2358, 2020.
16. Liu H, Lu X, Hu Y and Fan X: Chemical constituents of Panax ginseng and *Panax notoginseng* explain why they differ in therapeutic efficacy. Pharmacol Res 161: 105263, 2020.
17. Chang D, Liu J, Bilinski K, Xu L, Steiner GZ, Seto SW and Bensoussan A: Herbal medicine for the treatment of vascular dementia: An overview of scientific evidence. Evid Based Complement Alternat Med 2016: 7293626, 2016.
18. Feng L, Han F, Zhou L, Wu S, Du Y, Zhang D, Zhang C and Gao Y: Efficacy and safety of *Panax notoginseng saponins* (Xueshuantong) in patients with acute ischemic stroke (EXPECT) trial: Rationale and design. Front Pharmacol 12: 648921, 2021.
19. Chen M, Zhou SQ, Liu L, Wen YX and Chen LB: Notoginsenoside R1 alleviates the inflammation of osteoarthritis by activating the Nrf2/HO-1 signalling pathway in vitro and in vivo. J Funct Foods 85: 104666, 2021.
20. Wang M, Liu H, Xu L, Li M and Zhao M: The protective effect of notoginsenoside R1 on isoflurane-induced neurological impairment in the rats via regulating miR-29a expression and neuroinflammation. Neuroimmunomodulation 29: 70-76, 2022.
21. Hu T, Li S, Liang WQ, Li SS, Lu MN, Chen B, Zhang L, Mao R, Ding WH, Gao WW, *et al*: Notoginsenoside R1-induced neuronal repair in models of Alzheimer disease is associated with an alteration in neuronal hyperexcitability, which is regulated by Nav. Front Cell Neurosci 14: 280, 2020.
22. Wang X, Li B, Yu X, Zhou Y and Gao Y: The neuroprotective effect of GM-1 ganglioside on the amyloid-beta-induced oxidative stress in PC-12 cells mediated by Nrf-2/ARE signaling pathway. Neurochem Res 47: 2405-2415, 2022.
23. Cieślik M, Czapski GA and Strosznajder JB: The molecular mechanism of amyloid β42 peptide toxicity: The role of sphingosine kinase-1 and mitochondrial sirtuins. PLoS One 10: e0137193, 2015.
24. Gassowska M, Cieslik M, Wilkaniec A and Strosznajder JB: Sphingosine kinases/sphingosine-1-phosphate and death signalling in APP-transfected cells. Neurochem Res 39: 645-652, 2014.
25. Wang X, Wei L, Zhu J, He B, Kong B, Jin Y and Fu Z: Tetrabromoethylcyclohexane (TBECH) exhibits immunotoxicity in murine macrophages. Environ Toxicol 35: 159-166, 2020.
26. Ni L, Zhuge F, Yang S, Ma L, Zheng A, Zhao Y, Hu L, Fu Z and Ni Y: Hydrolyzed chicken meat extract attenuates neuroinflammation and cognitive impairment in middle-aged mouse by regulating M1/M2 microglial polarization. J Agric Food Chem 69: 9800-9812, 2021.
27. Livak KJ and Schmittgen TD: Analysis of relative gene expression data using real-time quantitative PCR and the 2(-Delta Delta C(T)) method. Methods 25: 402-408, 2001.
28. Ni Y, Ni L, Ma L, Wang Z, Zhao Y, Hu L, Zheng L and Fu Z: Neuroprotective effects of ProBeptigen/CMI-168 on aging-induced cognitive decline and neuroinflammation in mice: A comparison with essence of chicken. Acta Biochim Biophys Sin (Shanghai) 53: 419-429, 2021.
29. Ma L, Ni Y, Wang Z, Tu W, Ni L, Zhuge F, Zheng A, Hu L, Zhao Y, Zheng L and Fu Z: Spermidine improves gut barrier integrity and gut microbiota function in diet-induced obese mice. Gut Microbes 12: 1-19, 2020.
30. Qiao L, Chen Y, Dou X, Song X and Xu C: Biogenic selenium nanoparticles attenuate Aβ25-35-induced toxicity in PC12 cells via Akt/CREB/BDNF signaling pathway. Neurotox Res 40: 1869-1881, 2022.
31. Meng XL, Liu SY, Xue JS, Gou JM, Wang D, Liu HS, Chen CL and Xu CB: Protective effects of liensinine, isoliensinine, and neferine on PC12 cells injured by amyloid-β. J Food Biochem 46: e14303, 2022.
32. Li LX, Liu MY, Jiang X, Xia ZH, Wang YX, An D, Wang HG, Heng B and Liu YQ: Metformin inhibits $A\beta_{25-35}$-induced apoptotic cell death in SH-SY5Y cells. Basic Clin Pharmacol Toxicol 125: 439-449, 2019.
33. Avni D, Harikumar KB, Sanyal AJ and Spiegel S: Deletion or inhibition of SphK1 mitigates fulminant hepatic failure by suppressing TNFα-dependent inflammation and apoptosis. FASEB J 35: e21415, 2021.
34. Etemadi N, Chopin M, Anderton H, Tanzer MC, Rickard JA, Abeysekera W, Hall C, Spall SK, Wang B, Xiong Y, *et al*: TRAF2 regulates TNF and NF-κB signalling to suppress apoptosis and skin inflammation independently of Sphingosine kinase 1. Elife 4: e10592, 2015.
35. Wang XX, Tan MS, Yu JT and Tan L: Matrix metalloproteinases and their multiple roles in Alzheimer's disease. Biomed Res Int 2014: 908636, 2014.
36. LaFerla FM, Tinkle BT, Bieberich CJ, Haudenschild CC and Jay G: The Alzheimer's A beta peptide induces neurodegeneration and apoptotic cell death in transgenic mice. Nat Genet 9: 21-30, 1995.
37. Viola KL and Klein WL: Amyloid β oligomers in Alzheimer's disease pathogenesis, treatment, and diagnosis. Acta Neuropathol 129: 183-206, 2015.
38. Masliah E, Alford M, Adame A, Rockenstein E, Galasko D, Salmon D, Hansen LA and Thal LJ: Abeta1-42 promotes cholinergic sprouting in patients with AD and Lewy body variant of AD. Neurology 61: 206-211, 2003.

39. Kubo T, Nishimura S, Kumagae Y and Kaneko I: In vivo conversion of racemized beta-amyloid [(D-Ser 26)A beta 1-40] to truncated and toxic fragments [(D-Ser 26)A beta 25-35/40] and fragment presence in the brains of Alzheimer's patients. J Neurosci Res 70: 474-483, 2002.
40. Frozza RL, Horn AP, Hoppe JB, Simão F, Gerhardt D, Comiran RA and Salbego CG: A comparative study of beta-amyloid peptides Abeta1-42 and Abeta25-35 toxicity in organotypic hippocampal slice cultures. Neurochem Res 34: 295-303, 2009.
41. Varadarajan S, Kanski J, Aksenova M, Lauderback C and Butterfield DA: Different mechanisms of oxidative stress and neurotoxicity for Alzheimer's A beta(1-42) and A beta(25-35). J Am Chem Soc 123: 5625-5631, 2001.
42. Liu X, Ganguly P, Jin Y, Jhatro MJ, Shea JE, Buratto SK and Bowers MT: Tachykinin neuropeptides and amyloid β (25-35) assembly: Friend or foe? J Am Chem Soc 144: 14614-14626, 2022.
43. Wiatrak B, Kubis-Kubiak A, Piwowar A and Barg E: PC12 cell line: Cell types, coating of culture vessels, differentiation and other culture conditions. Cells 9: 958, 2020.
44. Gao X, Han Z, Huang C, Lei H, Li G, Chen L, Feng D, Zhou Z, Shi Q, Cheng L and Zhou X: An anti-inflammatory and neuroprotective biomimetic nanoplatform for repairing spinal cord injury. Bioact Mater 18: 569-582, 2022.
45. Changhong K, Peng Y, Yuan Z and Cai J: Ginsenoside Rb1 protected PC12 cells from $A\beta_{25-35}$-induced cytotoxicity via PPARγ activation and cholesterol reduction. Eur J Pharmacol 893: 173835, 2021.
46. Geng XD, Wang WW, Feng Z, Liu R, Cheng XL, Shen WJ, Dong ZY, Cai GY, Chen XM, Hong Q and Wu D: Identification of key genes and pathways in diabetic nephropathy by bioinformatics analysis. J Diabetes Investig 10: 972-984, 2019.
47. Gao JM, Zhang X, Shu GT, Chen NN, Zhang JY, Xu F, Li F, Liu YG, Wei Y, He YQ, *et al*: Trilobatin rescues cognitive impairment of Alzheimer's disease by targeting HMGB1 through mediating SIRT3/SOD2 signaling pathway. Acta Pharmacol Sin 43: 2482-2494, 2022.
48. Gao J, Yao M, Zhang W, Yang B, Yuan G, Liu JX and Zhang Y: *Panax notoginseng saponins* alleviates inflammation induced by microglial activation and protects against ischemic brain injury via inhibiting HIF-1α/PKM2/STAT3 signaling. Biomed Pharmacother 155: 113479, 2022.
49. Liu Y, Liu T, Ding K, Liu Z, Li Y, He T, Zhang W, Fan Y, Ma W, Cui L and Song X: Phospholipase Cγ2 signaling cascade contribute to the antiplatelet effect of notoginsenoside Fc. Front Pharmacol 9: 1293, 2018.
50. Du Y, Fu M, Wang YT and Dong Z: Neuroprotective effects of ginsenoside Rf on amyloid-β-induced neurotoxicity in vitro and in vivo. J Alzheimers Dis 64: 309-322, 2018.
51. Yan S, Li Z, Li H, Arancio O and Zhang W: Notoginsenoside R1 increases neuronal excitability and ameliorates synaptic and memory dysfunction following amyloid elevation. Sci Rep 4: 6352, 2014.
52. Ma B, Meng X, Wang J, Sun J, Ren X, Qin M, Sun J, Sun G and Sun X: Notoginsenoside R1 attenuates amyloid-β-induced damage in neurons by inhibiting reactive oxygen species and modulating MAPK activation. Int Immunopharmacol 22: 151-159, 2014.
53. Fricker M, Tolkovsky AM, Borutaite V, Coleman M and Brown GC: Neuronal cell death. Physiol Rev 98: 813-880, 2018.
54. Yoshiyama Y, Asahina M and Hattori T: Selective distribution of matrix metalloproteinase-3 (MMP-3) in Alzheimer's disease brain. Acta Neuropathol 99: 91-95, 2000.
55. Backstrom JR, Lim GP, Cullen MJ and Tökés ZA: Matrix metalloproteinase-9 (MMP-9) is synthesized in neurons of the human hippocampus and is capable of degrading the amyloid-beta peptide (1-40). J Neurosci 16: 7910-7919, 1996.
56. Ito S, Kimura K, Haneda M, Ishida Y, Sawada M and Isobe KI: Induction of matrix metalloproteinases (MMP3, MMP12 and MMP13) expression in the microglia by amyloid-beta stimulation via the PI3K/Akt pathway. Exp Gerontol 42: 532-537, 2007.
57. Lorenzl S, Buerger K, Hampel H and Beal MF: Profiles of matrix metalloproteinases and their inhibitors in plasma of patients with dementia. Int Psychogeriatr 20: 67-76, 2008.
58. Nübling G, Levin J, Bader B, Israel L, Bötzel K, Lorenzl S and Giese A: Limited cleavage of tau with matrix-metalloproteinase MMP-9, but not MMP-3, enhances tau oligomer formation. Exp Neurol 237: 470-476, 2012.
59. Poti F, Ceglarek U, Burkhardt R, Simoni M and Nofer JR: SKI-II-a sphingosine kinase 1 inhibitor-exacerbates atherosclerosis in low-density lipoprotein receptor-deficient (LDL-R-/-) mice on high cholesterol diet. Atherosclerosis 240: 212-215, 2015.
60. Lee JY, Han SH, Park MH, Baek B, Song IS, Choi MK, Takuwa Y, Ryu H, Kim SH, He X, *et al*: Neuronal SphK1 acetylates COX2 and contributes to pathogenesis in a model of Alzheimer's disease. Nat Commun 9: 1479, 2018.
61. Uddin MS and Lim LW: Glial cells in Alzheimer's disease: From neuropathological changes to therapeutic implications. Ageing Res Rev 78: 101622, 2022.
62. Cherifi C, Latourte A, Vettorazzi S, Tuckermann J, Provot S, Ea HK, Ledoux A, Casas J, Cuvillier O, Richette P, *et al*: Inhibition of sphingosine 1-phosphate protects mice against chondrocyte catabolism and osteoarthritis. Osteoarthritis Cartilage 29: 1335-1345, 2021.
63. Lai WQ, Irwan AW, Goh HH, Howe HS, Yu DT, Valle-Oñate R, McInnes IB, Melendez AJ and Leung BP: Anti-inflammatory effects of sphingosine kinase modulation in inflammatory arthritis. J Immunol 181: 8010-8017, 2008.